

Machine learning quantum mechanical ground states based on stochastic mechanics

Kai-Hendrik Henk^{*} and Wolfgang Paul

Physics Department, Martin-Luther-University Halle-Wittenberg, 06099 Halle, Germany



(Received 11 September 2023; accepted 20 November 2023; published 12 December 2023)

The Rayleigh-Ritz variation principle is a proven way to find ground states and energies for bound quantum systems in the Schrödinger picture. Advances in machine learning and neural networks make it possible to extend it from an analytical search from a subspace of the complete Hilbert space to the a numerical search in the almost complete Hilbert space. In this paper, we extend the Rayleigh-Ritz principle to Nelson's stochastic mechanics formulation of nonrelativistic quantum mechanics and propose an algorithm to find the osmotic velocities $u(x)$, which contain the information of a quantum systems in this picture. As a proof of concept, we calculated $u(x)$ for one-dimensional systems, the harmonic oscillator, the double well and the Pöschl-Teller potential. To obtain excited states, we calculate ground states of supersymmetrical partner Hamiltonians for each of these potentials. We will show that this method is more efficient than the stochastic optimal control algorithm that was the usual method to obtain osmotic velocities without going back to the Schrödinger equation.

DOI: [10.1103/PhysRevA.108.062412](https://doi.org/10.1103/PhysRevA.108.062412)

I. INTRODUCTION

Variation principles are one of the key building blocks of theoretical physics in all its areas. In nonrelativistic quantum mechanics this role is played by the Rayleigh-Ritz variation principle [1]. It tells us that, for a Hermitian operator \hat{H} , the lowest eigenvalue E_0 of its spectrum, and the corresponding eigenfunction ψ can be determined solving

$$E_0 = \min_{\psi} \frac{\langle \psi | \hat{H} | \psi \rangle}{\langle \psi | \psi \rangle}. \quad (1)$$

The solution ψ to this variation problem solves the stationary Schrödinger equation for the energy eigenvalue E_0 . It is well known that the Schrödinger equation is exactly solvable only for one- and two-particle problems and a few selected choices of potential. Beyond those, the Rayleigh-Ritz variation principle is a solid starting ground for approximations to both the ground-state energy and the ground-state wave function. This has been most highly developed for the solution of many particle problems, where the Rayleigh-Ritz principle underlies the proof of the Hohenberg-Kohn theorem and the development of density functional theory [2]. For not analytically solvable problems, the Rayleigh-Ritz principle provides an approximation strategy where the optimal solution is not searched for within the complete allowed Hilbert space, but only in a subspace of wave functions which can be parameterized by a few parameters [3]. With the rise of machine learning techniques it has, however, become possible to move from an analytical search in a restricted subspace to a numerical search in the almost (limited only by the practical implementation of the neural networks) complete Hilbert space [4,5].

In Nelson's stochastic mechanics formulation of non-relativistic quantum mechanics [6,7], variation principles

again played a central role in the formulation of the theory. Recently, a quantum Hamilton principle [8] could be used to derive quantum Hamilton equations of motion which can be used to solve a quantum problem without recourse to the Schrödinger equation [9–14]. The quantum Hamilton equations are coupled forward-backward stochastic differential equations which have to be solved numerically, and the standard algorithms for this are far less efficient than our tools for solving the Schrödinger equation. However, stochastic mechanics provides an alternative approach to the Rayleigh-Ritz principle as well. In stochastic mechanics all physical observables are stochastic variables and so is the total energy of the system. The expectation value of the stochastic variable energy agrees with the quantum mechanical expectation value of the energy operator and this can be used to formulate a Rayleigh-Ritz variation principle for the stochastic energy.

In the next section we will give some background on Nelson's stochastic mechanics, formulate the variation principle, and elucidate its relation to the standard version of the Rayleigh-Ritz principle. Section III will present an algorithm for solving this variation principle which is a machine-learning-based genetic algorithm. In Sec. IV we will discuss results for the ground state of selected one-dimensional quantum problems, and Sec. V will present results for the determination of excited states based on a supersymmetric (SUSY) factorization of the corresponding Hamiltonians. Finally, Sec. VI will present some conclusions and an outlook.

II. THEORETICAL BACKGROUND

The equations of motion of stochastic mechanics can be derived from a variation principle, the quantum Hamilton principle, similar to what one does in classical analytical mechanics. The general idea of this variation principle can be found in [6,8,12], we will use the formulation put forward by

^{*}kai-hendrik.henk@physik.uni-halle.de

Pavon [8]

$$J[\hat{v}, \hat{u}] = \min_v \max_u E \left\{ \int dt \left[\frac{1}{2} m [v(x, t) - iu(x, t)]^2 - V(x, t) \right] + \Phi_0 \right\}. \quad (2)$$

Here $v(x, t)$ is the velocity of the probability current, $u(x, t)$ the so-called osmotic velocity, $V(x, t)$ the potential, and Φ_0 a starting condition. This complex variation principle is a shorthand for two coupled variation principles which are encoded in the real and imaginary parts of the integral. The real part is a saddle-point action principle, the imaginary part a saddle-point entropy production principle [8]. They are saddle-point principles because the v player searches for a minimum while the u player searches for a maximum. The optimum for these jointly played games is the Nash equilibrium of this variation principle. Both velocities are gradients of scalar fields

$$v(x, t) = \frac{1}{m} \nabla S(x, t), \quad u(x, t) = \frac{\hbar}{2m} \nabla \ln[\rho(x, t)], \quad (3)$$

where $S(x, t)$ is the action and $\rho(x, t)$ the probability density of $x(t)$.

A. Stationary case

In the following we will consider the stationary case only, i.e., the quantum mechanical action is given by $S(x, t) = -Et$, where E is the energy of the system and limit ourselves to one-dimensional problems, which we will treat numerically later on. The above variation principle then simplifies to

$$J[u_0] = \max_u E \left\{ \int_0^T dt \left[-\frac{1}{2} mu^2[x(t)] - V[x(t)] \right] + S_0 \right\}, \quad (4)$$

which is equivalent to

$$J[u_0] = \min_u E \left\{ \frac{1}{T} \int_0^T dt \left[\frac{1}{2} mu^2[x(t)] + V[x(t)] \right] + S_0 \right\}, \quad (5)$$

by multiplication with $-1/T$. Here the E in front of the integral stands for building the expectation value and S_0 is a starting condition. The function u_0 obtained from this principle as the osmotic velocity of the ground state is an optimal feedback control. Using stochastic optimal control theory [9,15] to determine this feedback control results in coupled forward-backward stochastic differential equations

$$dx(t) = u_0[x(t)]dt + \sqrt{\frac{\hbar}{m}} dW_f(t), \quad t \in [0, T], \quad x(t=0) = x_0 \quad (\text{fixed}), \quad (6)$$

$$du_0[x(t)] = \frac{1}{m} V'(x(t))dt + \sqrt{\frac{\hbar}{m}} u'_0[x(t)]dW_b(t), \quad (7)$$

with x being the particle position, $dW_{f,b}$ a forward or backward in time Wiener process, and \hbar/m the diffusion coefficient. This is the stationary version of the quantum Hamilton equations which can be shown to be equivalent to the stationary Schrödinger equation using Itô calculus for the differential of the osmotic velocity [12,14]. The proof uses the fact that

the probability density of the process x is given by $\rho(x) = |\psi(x)|^2$.

The variation principle of Eq. (5) aims to find an osmotic velocity such that the expectation value of the time-averaged energy along a particle trajectory is minimized. The integrand is the stochastic energy of the particle $H(x) = 1/2 mu^2(x) + V(x)$, which is a fluctuating quantity whose average is equal to the quantum mechanical expectation value of the Hamiltonian in the ground state. Using the ergodicity of the Brownian diffusion in the ground state, this time-averaged energy is equal to the ensemble-averaged energy and we can write

$$J[u_0] = \min_u \int dx \rho(x) \left[\frac{1}{2} mu^2(x) + V(x) \right]. \quad (8)$$

The quantum Hamilton principle used for the derivation of the stationary quantum Hamilton equation is therefore equivalent to a Rayleigh-Ritz principle for the quantum mechanical ground state. The ground-state osmotic velocity u_0 gives rise to a ground-state density

$$\rho_0 = \exp \left\{ \frac{2m}{\hbar} \int^x u_0(x') dx' \right\}. \quad (9)$$

B. Relation to the standard Rayleigh-Ritz principle

For a normalized wave function, the Rayleigh-Ritz principle of Eq. (1) can be written as

$$E_0 = \min_{\psi} \langle \psi | \hat{H} | \psi \rangle,$$

and using the relation of the ground-state wave function to the ground-state density $\psi_0 = \sqrt{\rho}$ one obtains

$$\begin{aligned} E_0 &= \min_{\rho} \int dx \sqrt{\rho(x)} \left[-\frac{\hbar^2}{2m} \frac{d^2}{dx^2} + V(x) \right] \sqrt{\rho(x)} \\ &= \min_{\rho} \left\{ \int dx \left[\frac{1}{2} mu^2(x) + V(x) \right] \right. \\ &\quad \left. - \frac{\hbar^2}{2m} \int dx \frac{d^2 \rho}{dx^2} \rho(x) \right\} \\ &= \min_u \left\{ \int dx \left[\frac{1}{2} mu^2(x) + V(x) \right] \right. \\ &\quad \left. - \frac{\hbar^2}{4m} \int dx \frac{d^2 \rho}{dx^2} \rho(x) \right\}, \end{aligned} \quad (10)$$

where we employed the one-to-one correspondence between the density and the osmotic velocity. The first of these terms is just the Rayleigh-Ritz principle for Nelson's stochastic mechanics Eq. (8). The second term can be rewritten using

$$\frac{\hbar^2}{4m} \frac{d^2 \rho}{dx^2} = \left[mu^2 + \frac{\hbar}{2} \frac{du}{dx} \right] \rho, \quad (11)$$

and

$$\frac{m}{2} u^2 + \frac{\hbar}{2} \frac{du}{dx} = V - E. \quad (12)$$

With this, the second term is given by

$$\int dx \left[\frac{1}{2} mu^2(x) + V(x) - E \right] \rho(x), \quad (13)$$

which is exactly zero in the ground state. So the standard form of the Rayleigh-Ritz principle for the ground state of a quantum system is equivalent to the form derived from stochastic mechanics. However, we learned, in addition, that the standard form contains a term which actually does not contribute to the ground-state energy because it has to vanish in the ground state. This observation can be used for the formulation of a numerical approach presented in the next section

III. ALGORITHM

We propose now an algorithm that combines genetic algorithms with neural networks, which parametrize the osmotic velocity, with fitness functions from the Nelson picture. The inspiration was [16], where a similar one-phase algorithm was used to calculate optimal thermodynamic cycles under different restrictions and [4], where the stochastic gradient descends, deep learning and a class of variational problems were used to solve the Poisson equation.

A. Genetic algorithms

Genetic algorithms are a class of optimization algorithms that are inspired by evolution [17,18]. One has to initialize a population of individual solutions first. Those are evaluated by calculating their fitness using a scalar fitness function, which either has to be maximized or minimized. Then survivors are selected either randomly, with a calculated surviving probability depending on the individuals fitness, or deterministically, ergo a fixed number of best-performing individuals survive to the next generation. To repopulate the population, there exist two main methods of variation: crossover and mutation. Crossover takes, most of the time, two survivors and takes their genomes, their parametrization, and combines them to two new individuals. Mutation takes the genomes of one individual and changes some parameters either by replacing them with a completely new number or by adding or subtracting a random number obeying some distribution, e.g., a Gaussian or Cauchy distribution. The survivors and the new individuals are the population of the next generation and the cycle of selection and repopulation with genome variation continues until some convergence or abort criterion is fulfilled.

Genetic algorithms have the advantage over gradient-based methods [19] that they rarely, if at all, can get stuck in some local extrema of the fitness landscape. They are also easy to program and to understand.

B. Neural networks

Neural networks, which are used in almost all areas of science today, are of interest here because of their use as almost universal function approximation tool. For our purposes, only the forward path of a neural network is of interest. The normal way by back-propagation and stochastic gradient descent is substituted by the genetic algorithm.

A neural network is built from layers of neurons. Each one takes the output from each neuron of the previous layer and performs a weighted sum, which then is put into an activation

function ϕ (which typically has a sigmoidal form)

$$o_j = \phi \left(\sum_i w_{ij} o_i + b_{ij} \right) \quad (14)$$

form the input to the output layer.

For our algorithm, a four-layer neural network was used with n hidden neurons per hidden layer and one-neuron input and output layers and with tanh as activation function between every layer, except the second hidden layer and the output layer, where no activation function was used.

C. Setup of the algorithm

The algorithm has two phases which differ in the used fitness functions. The first one uses Eq. (10) to determine E_0 and a first estimate for u_0 ,

$$f_1 = \int \left(\frac{m}{2} u^2 + V \right) \rho dx + \left| \frac{\hbar^2}{4m} \frac{\int \rho'' dx}{\int \rho dx} \right| \rightarrow E_0, \quad (15)$$

and the second [20] uses Eq. (12) and E_0 from the first phase to improve the estimate for u_0

$$f_2 = \frac{m}{2} u^2 + \frac{\hbar}{2} \frac{\partial}{\partial x} u - V + E_0 \rightarrow 0. \quad (16)$$

It is advantageous to use two phases because of the properties of the two fitness functions. In f_1 both terms contain the probability density ρ . Because of this, the osmotic velocity is well approximated where ρ is large, but relatively poorly approximated where ρ is very small.

f_2 has the problem that E_0 is not *a priori* known but the advantage that ρ does not appear. In fact, with E_0 given, Eq. (12) is the Riccati equation for the ground state of the problem, which is equivalent to the stationary Schrödinger equation.

Having both phases in the algorithm cancels the problems of each individual fitness function. Having only one phase results in the activation function [here tanh(x)] determining the results in the area with small probability density (see subplot in Fig. 3). We employed Gaussian mutation which works by randomly picking biases and weights from a neural network and adding a $\mathcal{N}(0, 1)$ -distributed random number multiplied by a learning rate, lr. The selection of survivors in each generation is done by checking for the minima of f_1 and f_2 , respectively, in each phase. This is repeated until convergence, which is reached by having no improvement in the survivors for ten generations.

After convergence, the final osmotic velocity is used with Eq. (10) to obtain the final ground-state energy E_0 . This is done to gain consistency, i.e., that the final $u(x)$ fits to the final E_0 . It has to be mentioned that the difference between this final value and the one obtained after phase one is of the order of the relative error (Table I), which is expected considering Eq. (16) can be interpreted as varying the osmotic velocity to make it fit better to the E_0 obtained in phase one.

D. Discussion of hyperparameters and parameters

This algorithm contains a set of hyperparameters (to be differentiated from the weights and biases of the neural network, which typically are called the parameters of the

TABLE I. Correct and calculated ground-state energies for the three potentials with relative error in reduced units.

Potential	Correct E_0	Calculated E_0	Relative error
HO	0.5	0.50007	0.014%
PT	-4.5	-4.49939	0.0135%
DW	1.10342 [10]	1.10337	0.00453%

network), which can be adjusted to optimize the algorithm. Generally the learning rate should be small and the population size should be rather high because, if chosen too small, the algorithm converges too quickly to find a satisfying approximation. In practice, a learning rate of $lr = 0.001$ was found useful. Larger values resulted in large deviations in the energy error, mean absolute error (MAE) $\Delta_{MAE} = \frac{1}{N} \sum_{i=1}^N |x_i - \hat{x}_i|$ and root mean square error (RMSE) $\Delta_{RMSE} = \frac{1}{N} \sqrt{\sum_{i=1}^N (x_i - \hat{x}_i)^2}$ with respect to the reference curves. With the other hyperparameters fixed, a decrease of magnitude in the learning rate resulted in a decrease of magnitude in the MAE and RMSE (Fig. 1). The population size should not be smaller than 100. Larger populations improve the results, but an increase in order of magnitude did not have the same improvement in the errors (Fig. 1). The 25% survivor rate was chosen because an increase did not result in a increase in accuracy, but lowering the rate did result in lower accuracy. So, at least for these problems, 25% were optimal.

Regarding the architecture, two hidden layers were sufficient for these problems with no significant improvement with a third hidden layer added to the architecture.

For the number of neurons n , experience showed that for the harmonic oscillator and the Pöschl-Teller potential $n = 7$ was adequate. For the double-well potential $n = 25$ was used.

IV. RESULTS FOR THE GROUND STATE

To test the algorithm we used the harmonic oscillator, the symmetric Pöschl-Teller potential, and the double-well potential

$$V_{HO}(x) = \frac{\omega^2 m}{2} x^2, \quad (17)$$

$$V_{PT}(x) = -\frac{\hbar^2}{2mx_0^2} \frac{l(l+1)}{\cosh(x/x_0)^2}, \quad (18)$$

$$V_{DW}(x) = \frac{V_0}{x_0^4} (x^2 - x_0^2)^2, \quad (19)$$

respectively, with l being the number of bound states in the Pöschl-Teller potential, V_0 being the height of the barrier, and x_0 being the locations of the minima of the double well (see Fig. 2). For the numerical implementation, dimensionless units were used for the harmonic oscillator and the Pöschl-Teller potential. For the double well $V_0 = 2$ and $x_0 = 1.5$ were used.

The harmonic oscillator is the standard problem in physics. In quantum mechanics, the harmonic oscillator is exactly solvable with equidistant energy values

$$E_n = \hbar\omega\left(n + \frac{1}{2}\right), \quad n = 0, 1, 2, \dots, \quad (20)$$

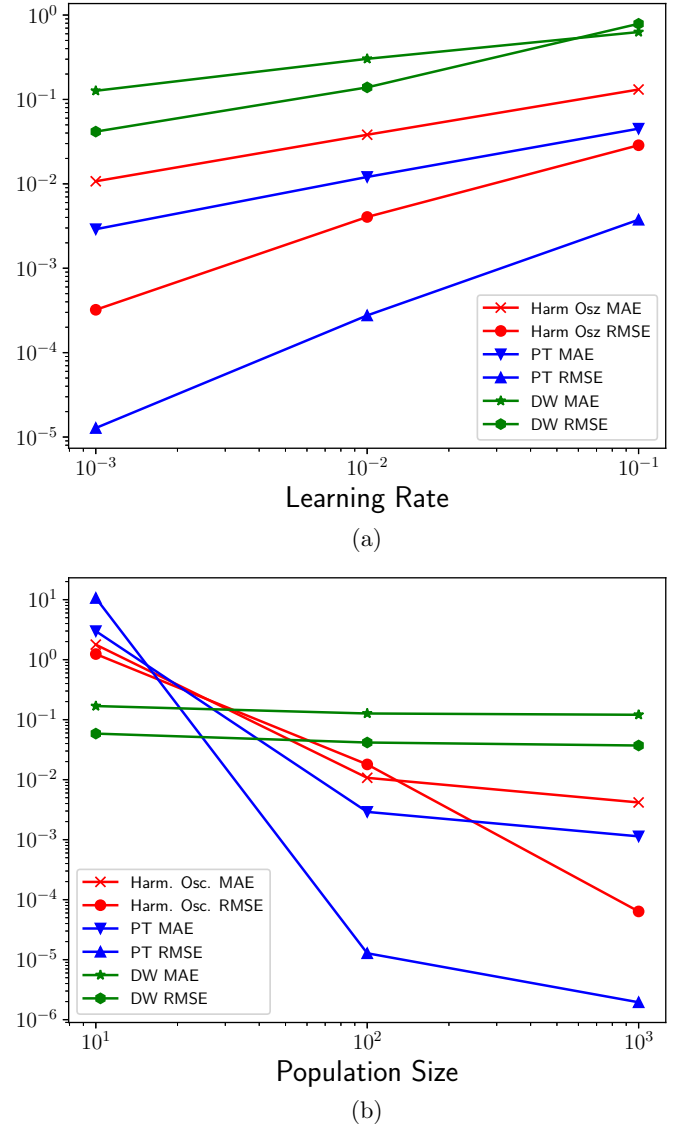


FIG. 1. RMSE and MAE change for the different potentials for increase in learning rate (top) and population size (bottom).

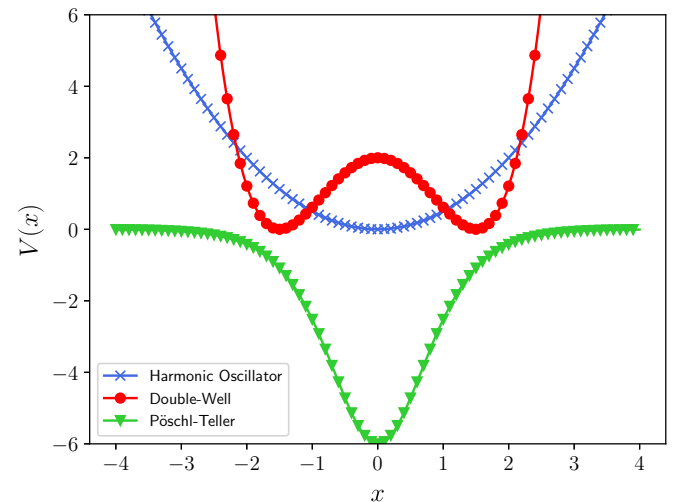


FIG. 2. The harmonic oscillator and the Pöschl-Teller potential in reduced units and the quartic double-well potential.

which makes it a good problem to test numerical methods against. In reduced units, the osmotic velocity for the harmonic oscillator is

$$u_{\text{HO}}(x) = -x. \quad (21)$$

The symmetrical Pöschl-Teller potential, used to describe two-atom systems, is also analytically solvable [21]. The wave functions are the Legendre polynomials $P_l^\mu[\tanh(x)]$ with l being the number of bound states and μ being the index of the bound state [22]. The energy spectrum is given by

$$E_{PT}^\mu = -\frac{\hbar^2 \mu^2}{2m} \quad \mu = 1, 2, \dots, l-1, l. \quad (22)$$

Using Eq. (3) with $\rho(x) = \Psi(x)^2 = P_l^\mu[\tanh(x)]^2$ the reference osmotic velocity for this potential was calculated.

The quartic double-well potential is only numerically solvable. Another property of it is that the gradient descent methods fail in solving it, making it a good potential to test other kinds of algorithms. The reference was created by solving the Schrödinger equation using the Numerov method [23,24] and again using Eq. (3) to obtain the osmotic velocity from the wave function.

The accuracy of the curves (e.g., Fig. 3) of the osmotic velocities fit very well with the errors, MAE and RMSE, which are of the order 10^{-4} to 10^{-5} , respectively, for the right choice of hyperparameters (Fig. 1).

The probability densities (Fig. 4) are approximated using Eq. (9).

The correct energies for the different potentials with these parameters can be seen in Table I. The calculated energies agree well with the correct energies with very small relative errors.

With respect to the numerical solution of the stochastic differential equations obtained using stochastic optimal control theory (STOC), one can also see an improvement regarding time efficiency. The STOC algorithm is quite slow, even for simple potentials with a few hours of calculation time. Here, for the Pöschl-Teller and the harmonic oscillator potentials, equally well-converged results were obtained in 15 to 20 minutes.

V. EXITED STATES

As shown in [25], the SUSY partner Hamiltonians can be derived to be given by

$$\hat{H}_n = T + V_0 - \sum_{i=0}^{n-1} \frac{\partial}{\partial x} u_i. \quad (23)$$

The ground-state energy of the first partner Hamiltonian has the energy of the first excited state of the original Hamiltonian, the ground state of the second partner Hamiltonian has the same energy as the second excited state of the original Hamiltonian, and so on. At each stage we have to solve the Rayleigh-Ritz principle for the respective Hamiltonian to obtain the corresponding ground-state osmotic velocity of the n th partner Hamiltonian.

This has to be done because the “normal” exited states have corresponding osmotic velocities with singularities in them. In Schrödinger quantum mechanics, the exited states

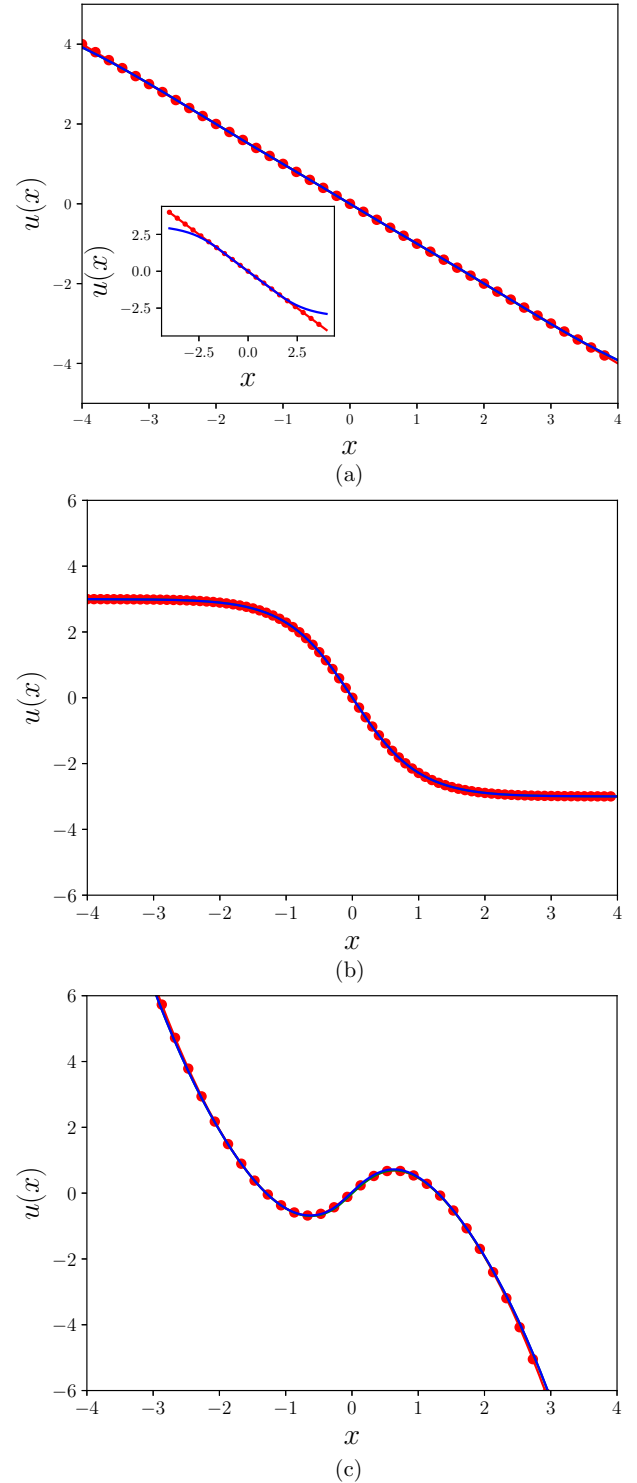


FIG. 3. Osmotic velocities of the harmonic oscillator (top), Pöschl-Teller (middle), and double-well (bottom) potential. All figures use reduced units. Visually, there is no difference between the references (connected red dots) and the solutions of the algorithm (continuous blue lines).

wave functions have nodes. There the probability distribution becomes zero and because of Eq. (3), there are singularities in the osmotic velocity. Because the ground states of the SUSY

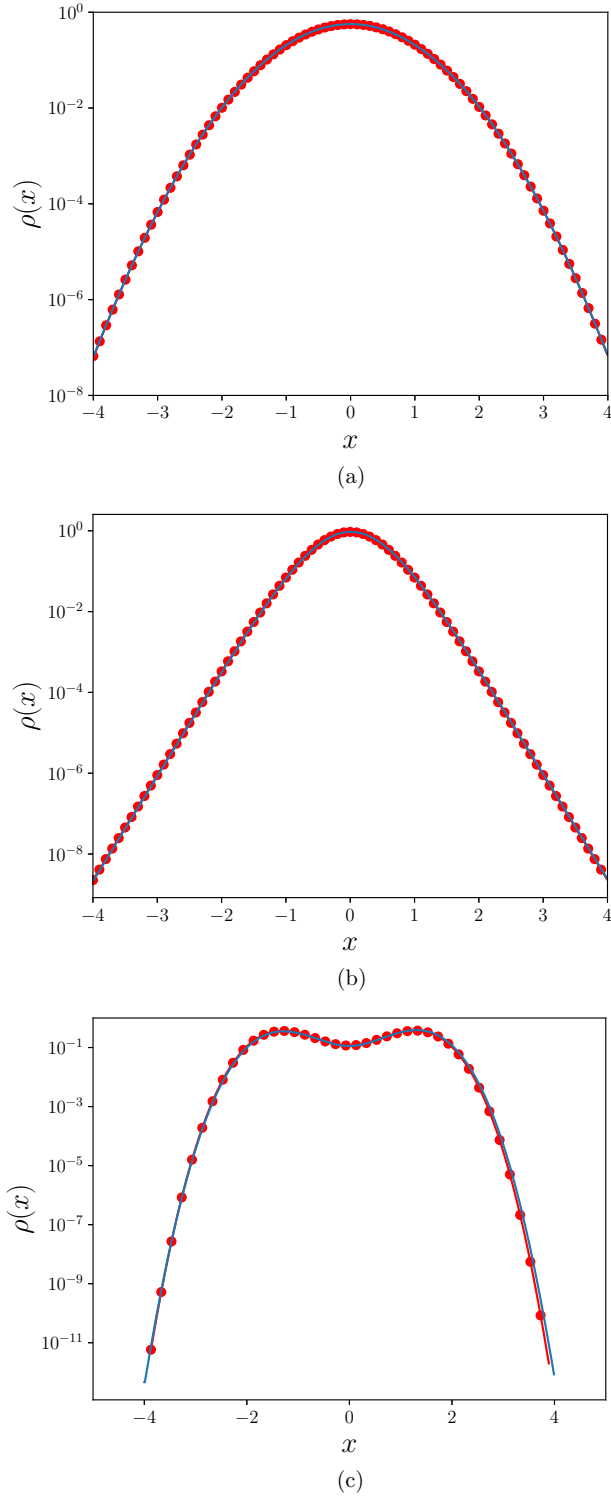


FIG. 4. Probability densities of the harmonic oscillator (top), Pöschl-Teller (middle), and double-well (bottom) potential. All figures use reduced units. No visible difference between the references (connected red dots) and the calculations from the newly calculated osmotic velocities (continuous blue) Eq. (9) exists.

partner Hamiltonians are nodeless, they are used to obtain the excited states.

For a broad region of coordinate space, the algorithm can approximate the ground states for the partner Hamiltonians

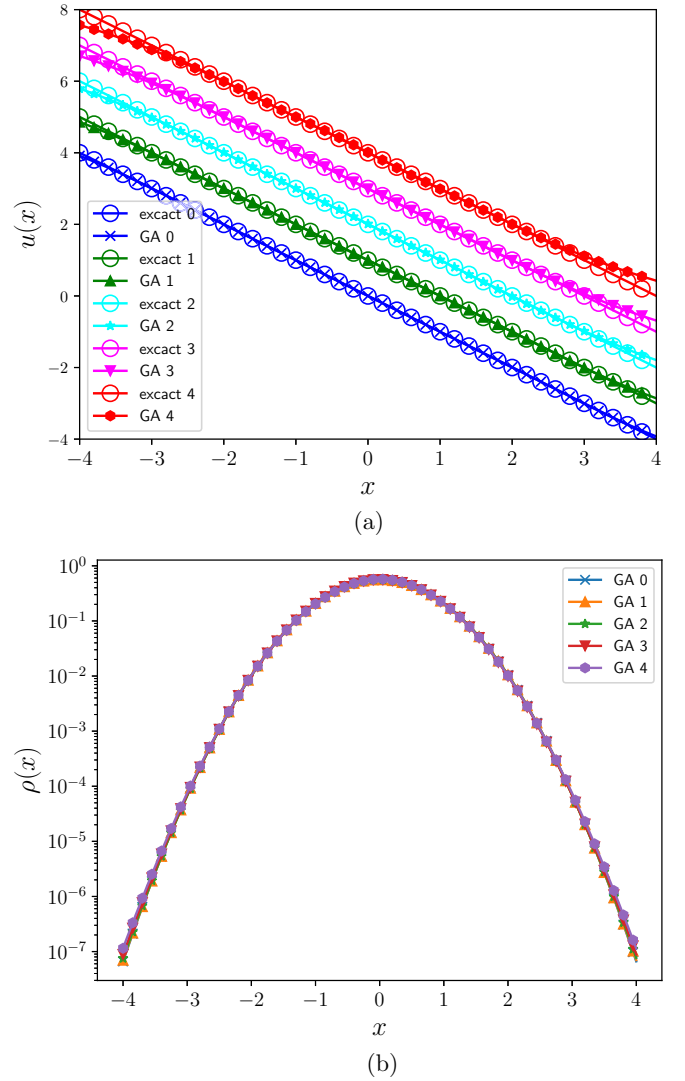


FIG. 5. Osmotic velocities for the first four excited states and the ground state of the harmonic oscillator, separated by ΔE (for visibility) (top) and corresponding probability densities (bottom) (GA N indicates the result of the genetic algorithm for the ground state $N = 0$ and the N th excited state). One can observe the growing error in the osmotic velocity from excitation to excitation. This has only very small influence on the error in the corresponding probability densities.

satisfactorily. The numerical uncertainties for the higher-order excited states arise from the sum of the (numerical) derivatives of the osmotic velocities. These propagate smaller errors to the next iteration of the algorithm, which increases the error from state to state. This happens independent from the hyperparameters used in the algorithm.

The harmonic oscillator is a good potential, where this can be observed, because the Hamiltonian only changes by a constant $-\nabla u(x) = -\nabla(-x) = 1 = \Delta E$ between excited states, with the osmotic velocity being left unchanged. In Fig. 5 one can see the growing error in the osmotic velocity very well. But the error in the corresponding probability densities (unchanged from state to state) is very small. This error can also be seen in (Fig. 6) as the slight rightwards drift of the

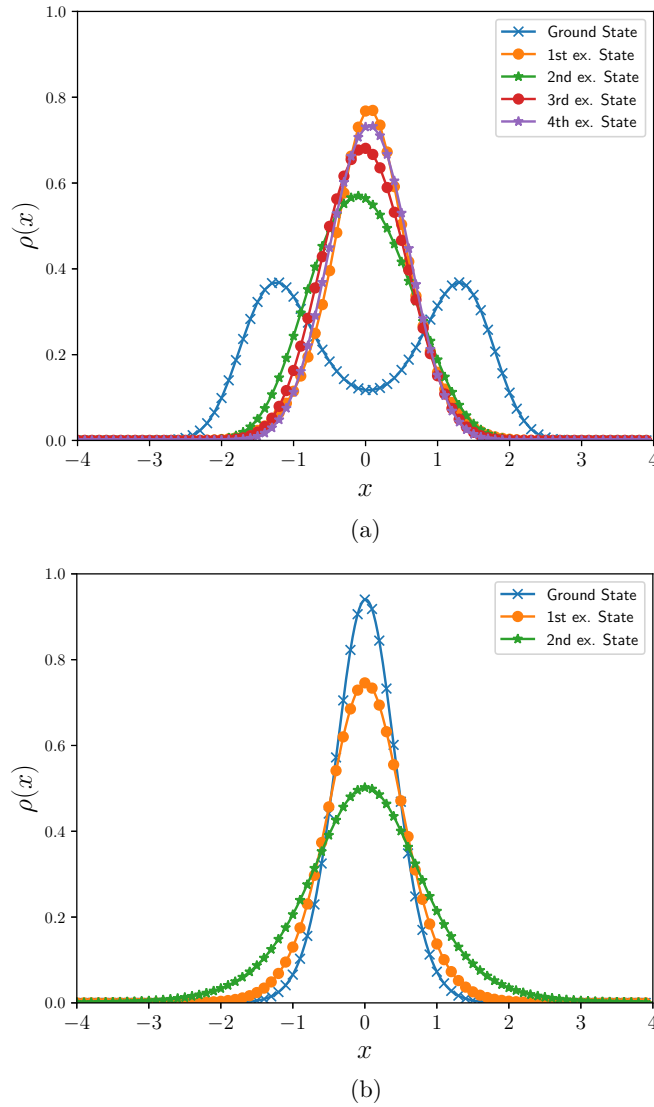


FIG. 6. Densities for the first four excited states and the ground state for the double well (top) and the first two excited states and the ground state of the Pöschl-Teller potential (bottom). One can observe that the error of the numerical calculation of the divergence in (23) propagates and grows with each excitation resulting in a slight shift of the symmetry axis of the densities (should be at $x = 0$).

center of the probability densities of the higher excited states, which should be at $x = 0$ because of the symmetry of the potential.

VI. CONCLUSION

We showed that the Hamilton principle of stochastic mechanics for a stationary state is equivalent to the Ritz variation principle of standard quantum mechanics. One can determine the ground-state probability (or, equivalently, the osmotic ground-state velocity of stochastic mechanics) by minimizing the expectation value of a stochastic Hamiltonian. We showed how to apply this to the ground state, and using the SUSY factorization of one-dimensional quantum problems, the excited states of one-dimensional systems. For this we introduced

a machine learning algorithm within a genetic optimization approach.

The algorithm offers an efficient way to numerically solve for the ground state of quantum problems. The resulting ground-state probability density can easily be determined over many orders of magnitude. With respect to its application within stochastic mechanics, it offers a much more efficient way to numerically solve for the ground state than what is possible via solution of the coupled forward-backward SDE derived from optimal control theory. We checked for accuracy and efficiency of the algorithm as a function of its free parameters and suggested an optimal compromise.

While we restricted our analysis to one-dimensional problems, an extension to two- or three-dimensional problems seems possible based on the simulation efficiency found so far. However, as with many machine learning applications, our approach faces the curse of dimensionality, making the possibility to extend it to many-particle physics problems questionable [at least working with the Riccati equation, i.e., the stationary Schrödinger equation of Eq. (12)]. These systems can be much more efficiently handled by methods based on discrete variable representations of the Schrödinger equation.

APPENDIX A: WORKFLOW OF THE ALGORITHM

The first algorithm works as follows.

- (1) Initialize 100 NNs using uniform distribution $([-1, 1])$.
- (2) Repeat until the energy does not decrease for ten generations:

- (a) calculate f_1 for each NN;
- (b) pick the 25 best NNs, discard the rest;
- (c) create 75 new NNs by copying randomly from the pool of survivors and mutate these copies with Gaussian mutation.

Thus one obtains a population of well-performing neural networks and the ground-state energy. The second phase is needed to get good results in the areas with small $\rho(x)$. Thus the second phase is as follows.

- (1) Pick the survivors of phase 1 and repopulate.
- (2) Repeat until the term f_2 does not decrease for ten generations:

- (a) calculate f_2 for each NN;
- (b) pick the 25 best NNs, discard the rest;
- (c) create 75 new NNs by copying randomly from the pool of survivors and mutate these copies with Gaussian mutation.

This has to be completed to get good results for $u(x)$.

APPENDIX B: UNITS

For the implementation, dimensionless units were used for the harmonic oscillator and the Pöschl-Teller potential derived from

$$E_{\text{HO}} = \frac{m}{2} u(x)^2 + \frac{m\omega^2}{2} x^2, \quad (\text{B1})$$

$$\frac{E}{\hbar\omega} = \frac{1}{2} \frac{m}{\hbar\omega} u(x)^2 + \frac{1}{2} \frac{m\omega}{\hbar} x^2, \quad (\text{B2})$$

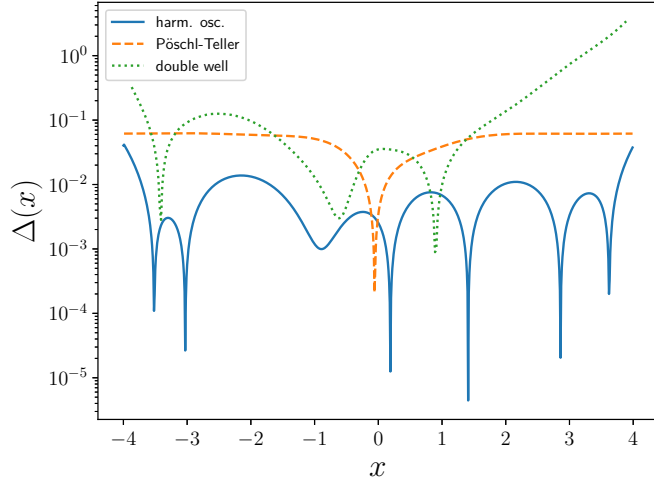


FIG. 7. Relative error of the probability densities from the corresponding references of the harmonic oscillator (blue continuous line), double well (green dotted line), and the Pöschl-Teller potential (orange dashed line). One can observe generally small deviations from the references.

resulting for the harmonic oscillator

$$\sqrt{\frac{m\omega}{\hbar}}x \rightarrow x, \quad \sqrt{\frac{m}{\hbar\omega}}u \rightarrow u, \quad \frac{E_{\text{HO}}}{\hbar\omega} \rightarrow E_{\text{HO}}, \quad (\text{B3})$$

and

$$E_{\text{PT}} = \frac{m}{2}u(x)^2 - \frac{\hbar^2}{2mx_0^2} \frac{l(l+1)}{\cosh(x/x_0)^2}, \quad (\text{B4})$$

$$\frac{2mx_0^2}{\hbar^2}E_{\text{PT}} = \frac{1}{2} \frac{2m^2x_0^2}{\hbar^2}u(x)^2 - \frac{l(l+1)}{\cosh(x/x_0)^2}, \quad (\text{B5})$$

resulting for the Pöschl-Teller potential

$$\frac{x}{x_0} \rightarrow x, \quad \frac{\sqrt{2}mx_0}{\hbar}u \rightarrow u, \quad \frac{2mx_0^2E_{\text{PT}}}{\hbar^2} \rightarrow E_{\text{PT}}. \quad (\text{B6})$$

For the double well

$$V_0 = 2, \quad x_0 = 1.5 \quad (\text{B7})$$

was used.

APPENDIX C: ERRORS

To aid in the visibility of the difference between the result of the algorithm and the references, we plotted the relative error of the probability densities

$$\Delta(x) = \frac{\rho(x) - \rho_{\text{ref}}(x)}{\rho_{\text{ref}}(x)}, \quad (\text{C1})$$

respectively (see Fig. 7). The error of the probability density is larger the further away we go from $x = 0$. The downward spikes are due to tanh activation function only sparsely hitting the references.

APPENDIX D: HARD- AND SOFTWARE IMPLEMENTATION

The algorithm was programed with PYTHON 3.8 with the packages NUMPY and COPY for calculations and TIME, DATETIME, MATPLOTLIB, MULTIPROCESSING, and COPY for evaluations. The program was run on a Intel Core i7-10700 CPU @ 2.90GHz \times 16 on a Ubuntu 20.04.5 LTS 64 bit system using PyCharm Community Edition.

-
- [1] A. Messiah, *Band 1 Quantenmechanik* (De Gruyter, Berlin, 1991).
 - [2] S. Kvaal and T. Helgaker, Ground-state densities from the rayleigh-ritz variation principle and from density-functional theory, *J. Chem. Phys.* **143**, 184106 (2015).
 - [3] D. Kouri, T. Markovich, N. Maxwell, and E. Bittner, Supersymmetric quantum mechanics, excited state energies and wave functions, and the rayleigh-ritz variational principle: A proof of principle study, *J. Phys. Chem. A* **113**, 15257 (2009).
 - [4] W. Ee and B. Yu, The deep ritz method: A deep learning-based numerical algorithm for solving variational problems, *Commun. Math. Stat.* **6**, 1 (2017).
 - [5] V. Kůrková, Kolmogorov's theorem and multilayer neural networks, *Neural Netw.* **5**, 501 (1992).
 - [6] E. Nelson, Derivation of the schrödinger equation from newtonian mechanics, *Phys. Rev.* **150**, 1079 (1966).
 - [7] J. Köppe, M. Patzold, M. Beyer, W. Grecksch, and W. Paul, Quantum Hamilton equations from stochastic optimal control theory, in *Infinite Dimensional and Finite Dimensional Stochastic Equations and Applications in Physics*, edited by W. Grecksch and H. Lisei, (World Scientific, Signapore, 2020), pp. 213–250.
 - [8] M. Pavon, Hamilton's principle in stochastic mechanics, *J. Math. Phys.* **36**, 6774 (1995).
 - [9] J. Köppe, Derivation and application of quantum Hamilton equations of motion, Ph.D. thesis, 2018.
 - [10] J. Köppe, M. Patzold, W. Grecksch, and W. Paul, Quantum Hamilton equations of motion for bound states of one-dimensional quantum systems, *J. Math. Phys.* **59**, 062102 (2018).
 - [11] M. Beyer, M. Patzold, W. Grecksch, and W. Paul, Quantum hamilton equations for multidimensional systems, *J. Phys. A: Math. Theor.* **52**, 165301 (2019).
 - [12] M. Beyer and W. Paul, On the stochastic mechanics foundation of quantum mechanics, *Universe* **7**, 166 (2021).
 - [13] M. Beyer and W. Paul, Particle spin described by quantum hamilton equations, *Ann. Phys. (Leipzig)* **535**, 2200433 (2022).
 - [14] J. Köppe, W. Grecksch, and W. Paul, Derivation and application of quantum hamilton equations of motion, *Ann. Phys. (Leipzig)* **529**, 1600251 (2016).
 - [15] B. Øksendal, *Stochastic Differential Equations: An Introduction with Applications*, Vol. 82 (Springer, New York, 2000).
 - [16] C. Beeler, U. Yahorau, R. Coles, K. Mills, S. Whitlam, and I. Tamblyn, Optimizing thermodynamic trajectories using evolutionary and gradient-based reinforcement learning, *Phys. Rev. E* **104**, 064128 (2021).
 - [17] M. Mitchell, *An Introduction to Genetic Algorithms* (MIT Press, Cambridge, MA, 1998).

- [18] D. E. Goldberg, *Genetic Algorithms in Search, Optimization, and Machine Learning* (Addison-Wesley, New York, 1989).
- [19] C. Lema and A. Choromanska, Approximating ground state energies and wave functions of physical systems with neural networks, [arXiv:2011.10694](#), the Third Workshop on Machine Learning and the Physical Sciences (NeurIPS 2020).
- [20] B. P. van Milligen, V. Tribaldos, and J. A. Jiménez, Neural network differential equation and plasma equilibrium solver, *Phys. Rev. Lett.* **75**, 3594 (1995).
- [21] G. Pöschl and E. Teller, Bemerkungen zur quantenmechanik des anharmonischen oszillators, *Z. Phys.* **83**, 143 (1933).
- [22] F. Williams, *Topics in Quantum Mechanics*, Progress in Mathematical Physics (Birkhäuser, Boston, 2003).
- [23] J. M. Blatt, Practical points concerning the solution of the schrödinger equation, *J. Comput. Phys.* **1**, 382 (1967).
- [24] B. R. Johnson, New numerical methods applied to solving the one-dimensional eigenvalue problem, *J. Chem. Phys.* **67**, 4086 (1977).
- [25] M. Patzold, Excited states in Nelson's stochastic mechanics, Master thesis, 2018.